

A DFT and CASSCF Study of Photocycloaddition Reactions of Biradicals from 6-Amino-2-(3-thienoyl)-1,4-benzoquinone

Gitanjali Sharma,[1] Ignatious Abraham,[1] Ram T. Pardasani,*[1] Prasad V. Bharatam,[2] and Tulsi Mukherjee[3]

[1]Department of Chemistry, University of Rajasthan, Jaipur-302 055, India

[2]Department of Medicinal Chemistry, National Institute of Pharmaceutical Education and Research (NIPER), Sector-67, Mohali-160 062, India

[3]Chemistry Group, Bhabha Atomic Research Centre, Mumbai-400 085, India

Received April 1, 2009; E-mail: rtpardasani@gmail.com

DFT-B3LYP and CASSCF calculations have been performed using a 6-31G* basis set to study photocycloaddition reactions of biradicals, generated by irradiation of 6-amino-2-(3-thienoyl)-1,4-benzoquinone, with ethylene. The calculated parameters of biradicals and transition states have also been compared with ground state parameters to completely elucidate the reaction mechanism of [2 + 2] and [3 + 2] photocycloaddition reactions. Preference for a particular cycloaddition pathway is ascertained by the relative stability between initially formed triplet biradical and another triplet biradical formed by hydrogen shift.

Biradicals or biradicaloid species derived from quinones present fascinating chemistry.[1] Photochemical [2 + 2]- and [3 + 2]-cycloaddition reactions of quinones present very useful synthetic methods for preparing four-membered and five-membered rings respectively.[2,3] Diverse medicinal and biological properties[4,5] of 1,4-benzoquinones make them highly suitable substrates for such cycloadditions. A number of [2 + 2] photocycloaddition reactions which lead to oxetane species have been reported.[6,7] Recently Marminon et al.[8] have reported one-pot [3 + 2]-cycloaddition reaction of 1,4-benzoquinone and benzyl azide whereas Murphy and Neville[9] have carried out comparative study of [2 + 2] and [3 + 2] cycloaddition reaction of 1,4-benzoquinone with allylsilane.

Density functional methods provide detailed electronic structure of biradical generating species like 1,4-benzoquinones.[10–14] Most of these studies are limited to understanding the electronic structure of species rather than understanding the mechanism of the reaction. In previous papers we have reported exhaustive theoretical studies on a wide variety of thermal and photochemical cycloadditions which principally include the stereochemical course of [3 + 2]-cycloaddition reactions of azomethine ylides[15–17] and theoretical aspects of [4 + 2] cycloadditions[18,19] of hetero-1,4-benzoquinones. Encouraged by these results we have focused our attention on a comparative study of [2 + 2] and [3 + 2] photocycloaddition reactions of 6-amino-2-(3-thienoyl)-1,4-benzoquinone. The results are presented herein.

Computational Details

All the calculations have been carried out using Gaussian98[20] and MOPAC6[21] suites of programs. Harmonic vibration frequencies of all stationary points have been computed to characterize them as energy minima (all frequencies are real) or transition states (one and only one imaginary frequency). The molecular and transition state geometries for the reaction of 6-amino-2-(3-thienoyl)-1,4-benzoquinone, through various possible pathways, [3 + 2]/[2 + 2], with ethylene have been located using CASSCF and B3LYP methods, with a 6-31G* basis set. The active space used in the CASSCF calculations is discussed in detail at appropriate places in the succeeding section. Intrinsic reaction coordinate calculations have been carried out using B3LYP/6-31G* level on one of the transition states to confirm the reaction path. In the B3LYP calculations of an open shell system, spin unrestricted formalization has been used. For all the minima on the singlet potential energy surface, the calculated (s^2) values are close to 1.0, so they are pure singlet biradicals, the triplet stationary points have (s^2) values close to 2.0 as expected.

Results and Discussion

The first task was to choose a model quinone. Literature survey revealed that aminobenzoquinone moiety is a component of the molecular framework of several natural products, e.g., kinamycine, and streptovaricine.[22,23] Further, the [3 + 2] cycloadducts of such quinones may act as precursors toward mitomycin antibiotics.[24] It has also been reported[25] that the thienyl group is a pharmacologically active moiety and enhances antimicrobial and antibacterial activity of quinones. Keeping these features in mind the synthetically feasible model quinone **1** (Scheme 1) was selected for the present study.

To begin with we have examined the relative stability of the three products that may be formed by [3 + 2]/[2 + 2] photocycloaddition of quinone **1** in their ground state (Scheme 1). The results have been summarized in Table 1.

A careful look at Table 1 reveals that [3 + 2] photocycloadduct has highest stabilization energy as compared to the other two or in other words photocycloadduct **2** formed by [3 + 2]

Published on the web December 10, 2009; doi:10.1246/bcsj.82.1477

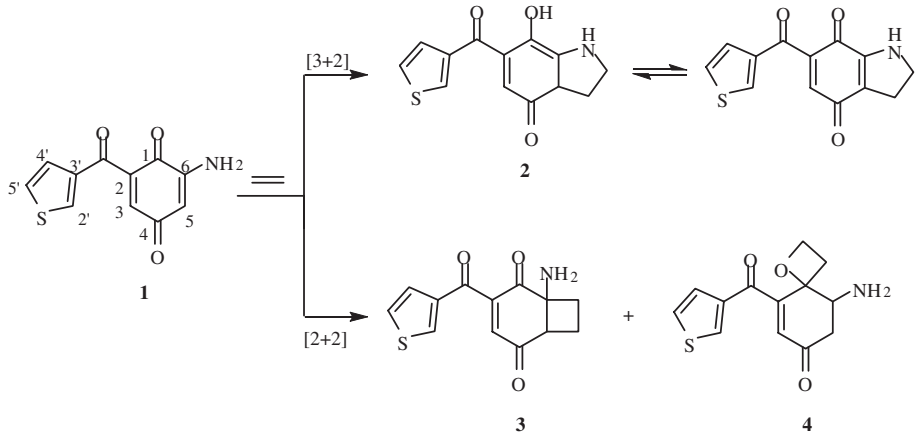

Scheme 1.

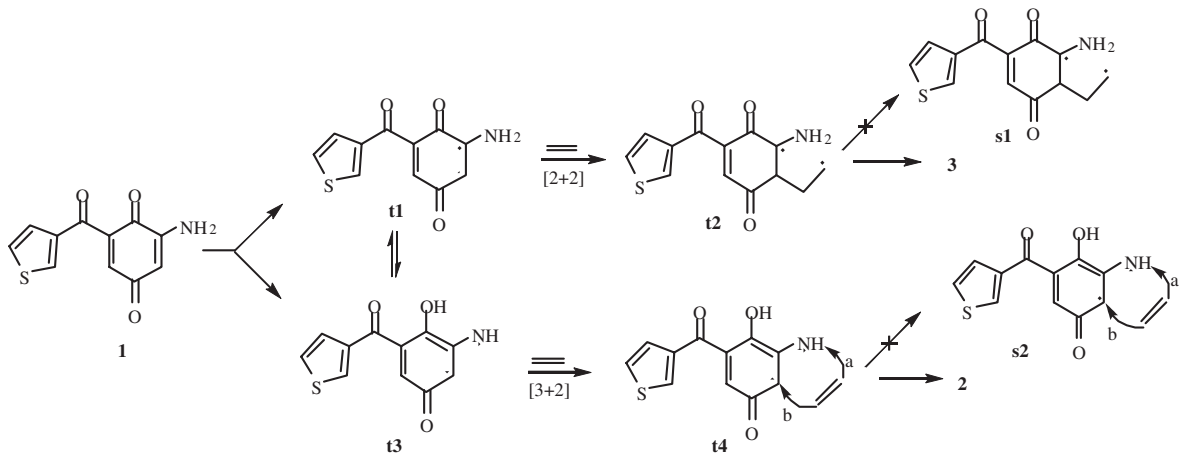

Scheme 2.

Table 1. Stabilization Energies[a)] of the Photocycloadducts of **1** with Ethylene Computed at B3LYP Level

Photocycloadducts	Stabilization energy
2	−20.7
3	−2.6
4	1.7

a) Relative to quinone **1** + **Ethylene** in kcal mol^{-1}.

photocycloaddition of ethylene on quinone **1** is the most stable and hence highly probable. Photocycloadduct **3** has stabilization energy lower than adduct **2**. Adduct **4** is less stable than the reactants which leaves its probability of formation negligible. Therefore, in the subsequent studies we focused on the comparative analysis of photocycloadducts **2** and **3** only assuming that formation of adduct **4** is not expected. Taking a clue from the initial ground state studies of photocycloadducts it was thought worthwhile to work on the course of reaction of adducts **2** and **3**. For this purpose calculations have been performed on all the intermediate biradicals and transition states involved.

Scheme 2 depicts the course of events that may take place between triplet **t1** and ethylene in [2 + 2] photocycloaddition and triplet **t3** and ethylene in [3 + 2] photocycloaddition reactions respectively. Once formed this triplet **t1** can either immediately decay to the ground state **1** through intersystem crossing or alternatively if its lifetime is long enough then it can react with ethylene to form corresponding triplet biradical **t2**. On the other hand, **t1** can undergo hydrogen hopping in the triplet state to **t3**. **t3** upon interaction with ethylene can follow two paths ("a" or "b") to finally produce a [3 + 2] cycloadduct **2**. The interconversion between **t1** and **t3** is the deciding factor in the selection of the final product. Figure 1 shows the optimized geometries of **1**, **t1**, and **t3** in three dimensions. In the triplet **t1**, the C1–O bond is elongated and C1–C2 bond is shortened with reference to its ground state **1**. Upon hydrogen hopping, C1–O(H) bond length gets elongated much prominently (0.09 Å) and the C1–C2 bond length shortened by 0.05 Å. The C2–N bond length remains unperturbed in the process **1** → **t1** → **t3**.

Additional structural isomers are possible for triplet **t3**. A detailed conformational analysis of four possible isomers of **t3** (Figure 2) was executed to find the most stable conformer. The DFT and CASSCF level of calculations were employed to find the energy of each conformation. Three different sets of active space are used to locate the excited triplet state stationary points of **t3** in CASSCF level calculations. The active space CASSCF (4,4) is composed of π and π^* orbitals of the newly formed C1–C2 π bond and σ and σ^* orbitals of C2–C3 bond. This active space is expanded to CASSCF (6,6) by including the σ

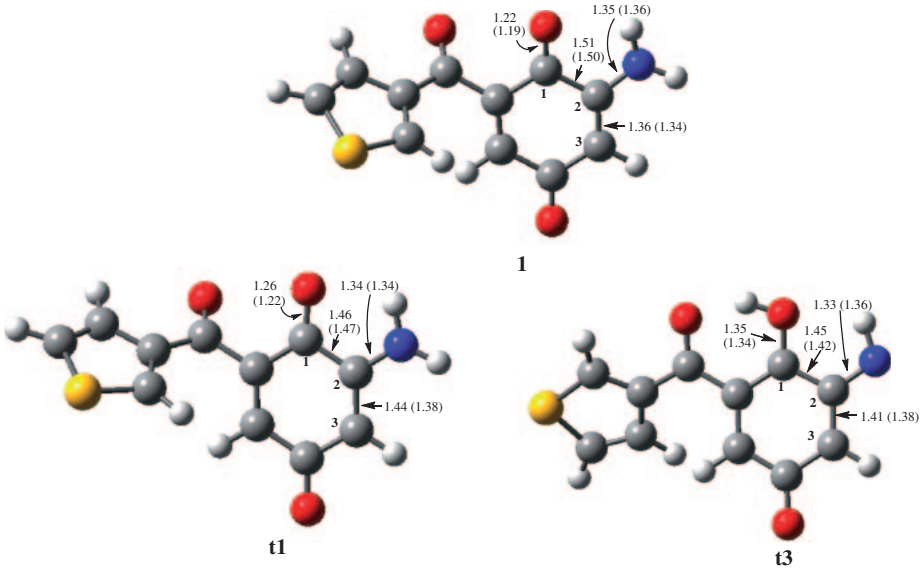

Figure 1. Optimized structures of the ground state **1** and $^3(\pi$–$\pi^*)$ excited states, **t1** and **t3** of 6-amino-2-(3-thienoyl)-1,4-benzoquinone. Selected bond distances obtained at the B3LYP (CASSCF) levels of calculation are shown in Å units. Atomic numbering scheme used in the discussion is shown in the figure.

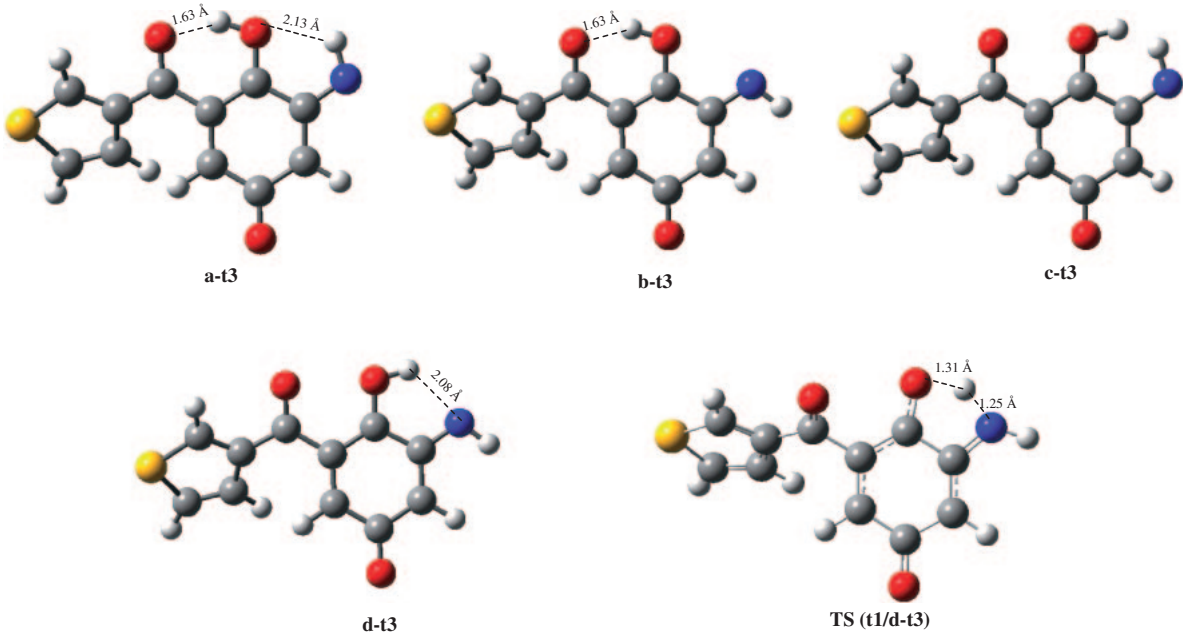

Figure 2. Different conformations of excited triplet **t3** and **t1/dt-3** transition state located at B3LYP/6-31G* level.

and σ^* orbitals of C1–O bonds. In order to correlate the effect of odd electrons the non-bonding orbitals in C3 and N carrying odd electrons are incorporated to further expand the active space to CASSCF (8,8). The results are summarized in Table 2.

It is quite clear from Table 2 that the conformer **a-t3** having low energy is the most stable in all cases. The greater stability of **a-t3** may be attributed to two intramolecular hydrogen bonds with 2.13 (NH···O) and 1.63 Å (OH···O) bond lengths (Figure 2). **b-t3** is less stable than **a-t3** by 2.5–3.2 kcal mol^{-1} (1 kcal mol^{-1} = 4.184 kJ mol^{-1}) in different levels of calculations since one hydrogen bond (NH···O) is removed. The possibility of any hydrogen bonding stabilization is hindered in

Table 2. Relative Energies (kcal mol^{-1}) of Conformations of **t3** Calculated at DFT-B3LYP and CASSCF Levels Using 6-31G* Basis Set

Conformation	Relative energy			
	DFT-B3LYP	CASSCF (4,4)	CASSCF (6,6)	CASSCF (8,8)
a-t3	0.00	0.00	0.00	0.00
b-t3	+2.50	+2.96	+2.96	+3.16
c-t3	+25.28	+29.23	+29.24	+26.60
d-t3	+8.41	+9.33	+9.31	+16.77

Table 3. Singlet–Triplet Excitation Energies (in kcal mol^{-1}) for Quinone **1** Computed with B3LYP and CASSCF Methods Using 6-31G* Basis Set

	ΔE	
	B3LYP	CASSCF(6,6)
1 → **t1**	36.48	59.37
1 → **t3**	30.62	52.56
t1 → **t3**	−5.86	−6.81

c-t3 and hence it is the least stable among the four conformations. Finally **d-t3** is more stable than **c-t3** but less stable than both **a-t3** and **b-t3**. **d-t3** is about 9 kcal mol^{-1} less stable than **a-t3**. The higher stability of **d-t3** than **c-t3** can be attributed to a weaker hydrogen bonding (OH···N) with 2.08 Å bond length. Subsequently further studies on triplet **t3** are performed on the most stable **a-t3** conformer. Hence **a-t3** is considered as **t3**. The **t1** → **a-t3** conversion does not follow a least motion pathway which eliminates the possibility of a transition state. However the **t1** → **d-t3** conversion occurs through a least motion pathway and a transition state is expected (Figure 2). The energy barrier for **t1** → **d-t3** is found to be 10.59 kcal mol^{-1} which is quite reasonable for such rearrangements and hence the **t1** → **d-t3** rearrangement is expected to takes place as a first step followed by rotation to give the most stable conformation **a-t3**.

The relative energies of singlet ground and triplet excited states of **1** are shown in Table 3. Considering the excited states, triplet **t3** is found to be more stable than **t1** according to both B3LYP/6-31G* method (−5.86 kcal mol^{-1}) and CASSCF/6-31G* method (−6.81 kcal mol^{-1}). This clearly indicates that there is a high probability of H-shift in **t1** to give **t3** in the triplet state. The estimated adiabatic singlet–triplet excitation energies for **1** → **t1** and **1** → **t3** are 36.48 and 30.62 kcal mol^{-1} at DFT-B3LYP/6-31G* and 59.37 and 52.56 kcal mol^{-1} respectively at CASSCF/6-31G* level.

The greater stability of **t3** relative to **t1** is well understood because of the two hydrogen bonds as described in the preceding paragraph. Once it was established that the two intermediates i.e., **t1** and **t3** (Figure 1) having only slight energy difference were possible for quinone **1**, it was envisioned that both the intermediates will lead to very different products and the mechanism of attack of ethylene on both of them will also be distinct. Hence, it was thought worthwhile to study the reaction pathways of these intermediates separately.

In the first part of our study intermediate **t1** has been selected. In this case attack of ethylene can take place on C2 as well as C3. But we have only considered the attack of ethylene on C3 of **t1**, since it has lower energy than C2 (calculations on triplet structures with initial attack on other possible α/β centers to carbonyl groups in **1** showed higher energies than C3 and they were not considered in the studies). When ethylene attacks this intermediate it can present several conformations arising from rotation around the newly forming C3–C4 bond. In particular we have considered the following conformers arising from the C2–C3–C4–C5 dihedral angle: anti (**t2a**, ψ around 180°), gauche-in (**t2g-in**, ψ around +60°), and gauche-out (**t2g-out**, ψ around −60°). The structures of the stationary points corresponding to these **t2** intermediates are shown in Figure 3. The potential energy barriers and reaction energies for the formation of intermediates involved in [2 + 2] photocycloaddition are calculated at DFT-B3LYP/6-31G* and CASSCF(6,6)/6-31G* levels. The active space CASSCF(6,6) is comprised of σ and σ^* orbitals of the newly formed C3–C4 bond along with the two orbitals in C2 and C5 containing the odd electrons and the σ and σ^* orbitals of C2–C3 bond. The results are tabulated in Table 4.

A study of Table 4 clearly indicates that the three conformers arising from the attack of ethylene on **t1** have comparable energies. All three structures of the intermediate are lower in energy compared to the starting material (**t1** + **Ethylene**) at B3LYP level, but at CASSCF level, the energies of the three intermediate structures are almost the same as the starting material. The structures of the transition states during the formation of the intermediates **t2a**, **t2g-in**, and **t2g-out** are also obtained and their structures are given in Figure 3 and the relative energies are given in Table 4. The observed C–C bond lengths during ethylenic attack are in the range of 2.15 Å. Both B3LYP as well as CASSCF studies reveal **t2g-out** to be a little more favorable than the other two.

In the second part of the study, the attack of ethylene to triplet **t3** (Scheme 2) leading to the formation of corresponding biradical **t4** has been taken into account. The attack can take place either on N of amino group (path "a") or on C3 atom (path "b") of **t3** to form corresponding **t4** biradicals. Here we have considered three conformations arising from the C2–N6–C4–C5 dihedral angle: anti (**a-t4a**, ψ around 180°), gauche-in (**a-t4g-in**, ψ around +60°), and gauche-out (**a-t4g-out**, ψ around −60°) for path "a." Similarly for path "b" the conformations arising from the C2–C3–C4–C5 dihedral angle are anti (**b-t4a**, ψ around 180°), gauche-in (**b-t4g-in**, ψ around +60°), and gauche-out (**b-t4g-out**, ψ around −60°). Calculations were performed on both pathways. The structures of the stationary points corresponding to these **t4** intermediates are shown in Figures 4a and 4b respectively for paths "a" and "b." The potential energy barriers and reaction energies for the formation of these **t4** intermediates are estimated. The active space CASSCF (6,6) was used for CASSCF calculations for path "a" comprised of σ and σ^* orbitals of the newly formed N6–C4 bond along with the two orbitals in C2 and C5 containing the odd electrons and the σ and σ^* orbitals of the C2–C3 bond. In path "b" calculations the σ and σ^* orbitals of the newly formed C3–C4 bond along with the two orbitals in C5 and N_6 containing the odd electrons and the σ and σ^* orbitals of the C2–C3 bond constitute the active space. The results are presented in Table 5.

As evidenced from Table 5 the energies associated with path "a" are less than those in path "b." On the basis of energy values path "a" is favored over path "b" which may be attributed to larger electron density on nitrogen in comparison to that on C3. The trends in the energies observed using B3LYP and CASSCF methods are quite similar, though the values are not directly matching. Both B3LYP as well as CASSCF studies reveal **t2g-out** to be the stable conformer.

Next it was thought worthwhile to study the singlet excited states of the above biradicals (**t2** and **t4**) as these triplet excited states may undergo intersystem crossing to the ground state

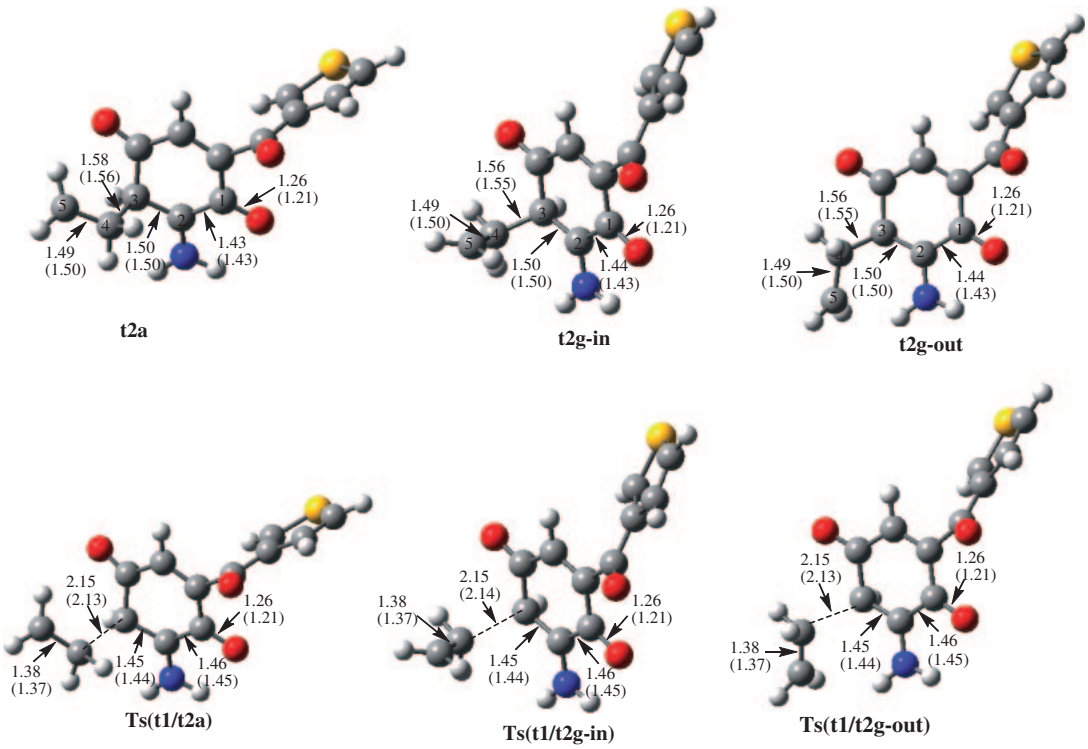

Figure 3. Structures of stationary points corresponding to the attack of ethylene to **t1** during [2 + 2] photocycloaddition. Selected interatomic distances obtained at the B3LYP (CASSCF) levels of calculation are given in Å units. Atomic numbering scheme used in the discussion is shown in the figure.

Table 4. Energies[a)] Computed at the B3LYP and CASSCF[b)] Levels of Calculation for Stationary Points[c)] Corresponding to the Attack of Ethylene to **t1**

	Relative energies	
	B3LYP	CASSCF
t2a	−7.6	1.4
t2g-in	−8.7	1.6
t2g-out	−10.6	2.2
TS (t1/t2a)	4.0	13.9
TS (t1/t2g-in)	3.9	13.5
TS (t1/t2g-out)	3.8	13.2
s1a	−3.8	18.3
TS (t1/s1a)	22.7	27.5

a) Relative to **t1** + **Ethylene** in kcal mol^{-1}. b) Six electrons in six orbitals. c) See Figure 3.

potential energy surface. We have optimized the geometries of singlet biradicals **s1** for [2 + 2] as well as biradicals **s2** for [3 + 2] photocycloaddition. The structures of selected **s1** and **s2** intermediates are depicted in Figure 5. Their energies (Tables 4 and 5) are much higher rather than being lower than the corresponding triplet biradicals energies i.e., **t2** energies for [2 + 2] and **t4** energies for [3 + 2] photocycloaddition reactions. As the energy required for intersystem crossing is in the range of 5–15 kcal mol^{-1}, intersystem crossing will not be allowed in the region of **t2** and **t4** intermediates. Transition states for these intermediates have also been located. The computed potential energy barriers are presented in Tables 4 and 5. Energy barriers are also very different for the two electronic states. Since the energy differences are very high for **s1** and **s2** biradicals, it is not possible for them to form expected products.

This leaves only one choice i.e., **t2** and **t4** biradicals may directly lead to the formation of products **3** and **2**. But these triplet biradical intermediates (**t2** and **t4**) can also undergo fragmentation to **t1** and ethylene. Hence these biradicals will probably follow that path which requires less energy. Fragmentation may take place from either a gauche or an anti conformer. But in this case the fragmentation energy barrier is close to 16–18 kcal mol^{-1}, which makes it a rather difficult process. In addition the adduct **2** once formed will immediately change to its stable tautomeric form making fragmentation a rather unlikely process.

Conclusion

6-Amino-2-(3-thienoyl)-1,4-benzoquinone was chosen for the present study as it proved to be a best model owing to its medicinal and pharmacological relevance. A detailed study of the ground and triplet excited state potential energy surfaces involved in [2 + 2] and [3 + 2] photocycloadditions of 6-amino-2-(3-thienoyl)-1,4-benzoquinone and ethylene reveal that out of three possible cycloadditions, only [2 + 2] cycloadduct (in which a cyclobutane ring is formed) and [3 + 2] are exothermic and have large stabilization energies while the [2 + 2] cycloadduct in which an oxetane ring is formed is endothermic thus leaving the possibility of its formation minimum. Therefore the two cycloadditions which showed larger stabilization energies were selected for further studies. Both [2 + 2] as well as [3 + 2] photocycloadditions were

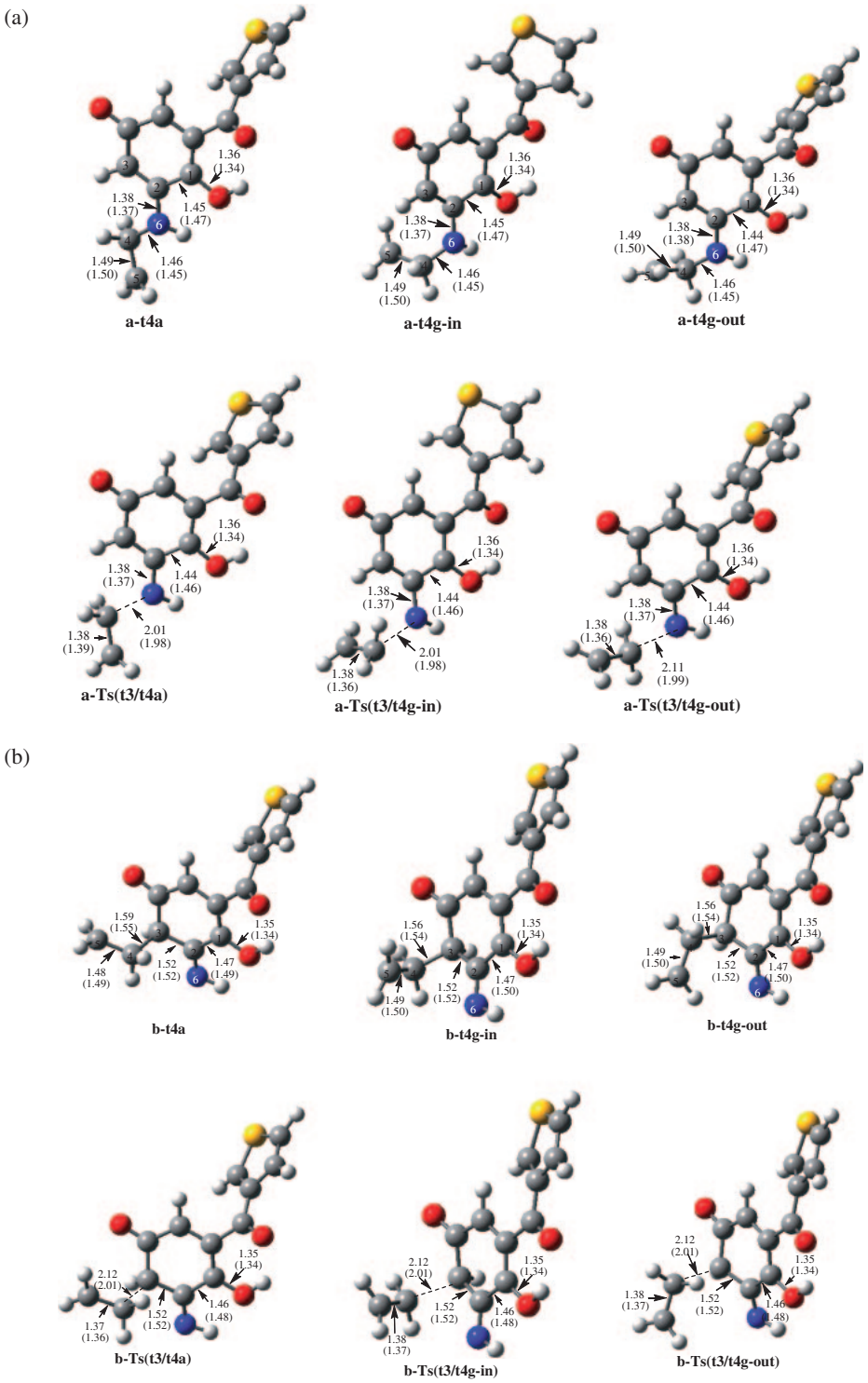

Figure 4. Structures of stationary points corresponding to the attack of ethylene on **t3**: (a) Path "a" and (b) path "b." Selected distances obtained at the B3LYP (CASSCF) levels of calculation are in Å units. Atomic numbering scheme used in the discussion is shown in the figure.

studied in their excited states. As the energy difference between **t1** and **t3** is much less, hydrogen shift may take place very efficiently. Both B3LYP as well as CASSCF calculations envisage gauche-out coformer to be more stable than the other two conformers in [2 + 2] as well as [3 + 2] photocycloadditions. In case of [3 + 2] photocycloaddition reaction the attack of ethylene on N as well as on C3 have been studied extensively and it has been found that lower energy is required when ethylene attacks N rather than C3. So addition of ethylene will probably occur on nitrogen. For all the biradicals, triplet as well as singlet state energies have been calculated and in each case singlet state energy is higher than the corresponding triplet

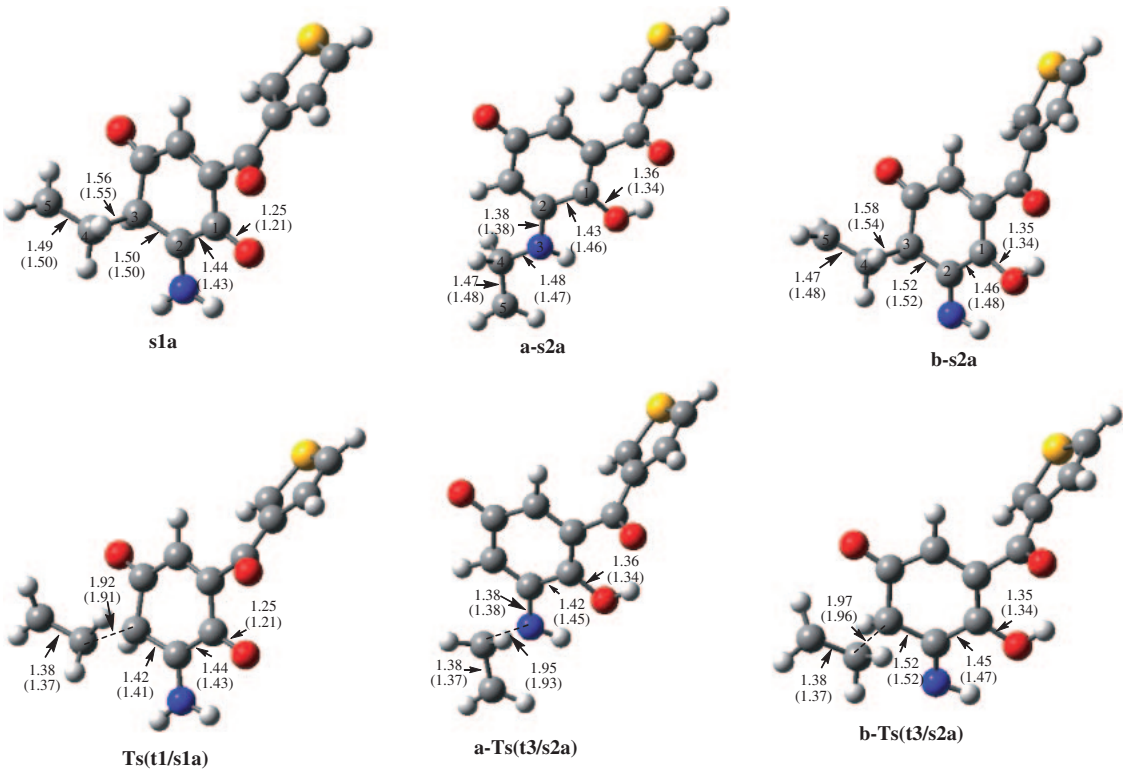

Figure 5. Structures of singlet biradicals corresponding to reaction between ethylene and 6-amino-2-(3-thienoyl)-1,4-benzoquinone.

Table 5. Relative Energies[a] Computed at the B3LYP and CASSCF[b] Level of Calculation for Stationary Points[c] Corresponding to the Attack of Ethylene on **t3**

	Relative energies	
	B3LYP	CASSCF
Path "a"		
a-t4a	−7.9	2.2
a-t4g-in	−8.1	2.4
a-t4g-out	−8.6	2.8
a-TS (t3/t4a)	9.2	16.0
a-TS (t3/t4g-in)	9.4	16.1
a-TS (t3/t4g-out)	9.5	16.3
a-s2a	−3.3	19.5
a-TS (t3/s2a)	23.1	28.7
Path "b"		
b-t4a	1.4	5.1
b-t4g-in	1.6	5.4
b-t4g-out	1.9	5.7
b-TS (t3/t4a)	14.5	18.4
b-TS (t3/t4g-in)	14.7	18.7
b-TS (t3/t4g-out)	14.9	18.8
b-s2a	5.7	21.1
b-TS (t3/s2a)	26.8	29.9

a) Relative to **t3** + **Ethylene** in kcal mol^{-1}. b) Six electrons in six orbitals. c) See Figure 4a for Path "a" and Figure 4b for Path "b."

state energy thus making intersystem crossing practically impossible. Thus it was predicted that triplet biradicals (**t2** and **t4**) might lead to the corresponding products (**3** and **2**). But the above biradicals can also undergo fragmentation back to the reactants. Therefore it was imperative to study the two competing processes i.e., cyclization and fragmentation. Theoretical results favor cyclization.

Financial assistance from DAE/BRNS is gratefully acknowledged. IA thanks CSIR, New Delhi for NET-SRF. The optimized geometries of discussed molecules may be obtained on request from the authors.

References

1 J. M. Bruce, in *Chemistry of Quinonoid Compounds Part 1*, ed. by S. Patai, Wiley, New York, **1974**, p. 465.

2 A. C. Weedon, in *Synthetic Organic Photochemistry*, ed. by W. M. Horspool, Plenum, New York, **1984**.

3 J. W. Lown, in *1,3-Dipolar Cycloaddition Chemistry*, ed. by A. Padwa, Wiley, New York, **1984**, p. 1.

4 D. Pockel, T. H. J. Niedermeyer, H. T. L. Pham, A. Mikolasch, S. Mundt, U. Lindequist, M. Lark, O. Werz, *Med. Chem.* **2006**, *2*, 591.

5 J. C. Lien, L.-J. Huang, J.-P. Wang, C.-M. Teng, K.-H. Lee, S.-C. Kuo, *Chem. Pharm. Bull.* **1996**, *44*, 1181.

6 D. Bryce-Smith, E. H. Evans, A. Gilbert, H. S. McNeill, *J. Chem. Soc., Perkin Trans. 2* **1991**, 1587.

7 K. A. Schnapp, R. M. Wilson, D. M. Ho, R. A. Caldwell, D. Creed, *J. Am. Chem. Soc.* **1990**, *112*, 3700.

8 C. Marminon, J. Gentili, R. Barret, P. Nebois, *Tetrahedron*

2007, *63*, 735.
9 W. S. Murphy, D. Neville, *Tetrahedron Lett.* **1997**, *38*, 7933.
10 Y. Song, J. Xie, H. Shu, G. Zhao, X. Lv, H. Cai, *Bioorg. Med. Chem.* **2005**, *13*, 5658.
11 S. H. Ma, X. D. Zhang, H. Xu, L. L. Shen, X. K. Zhang, Q. Y. Zhang, *J. Photochem. Photobiol., A* **2001**, *139*, 97.
12 R. Jacob, M. Puranik, J. Chandrasekhar, *Chem. Phys. Lett.* **1999**, *301*, 498.
13 A. Pawlukojć, I. Natkaniec, G. Bator, L. Sobczyk, E. Grech, J. Nowicka-Scheibe, *Spectrochim. Acta, Part A* **2006**, *63*, 766.
14 Y. Song, J. Xie, Y. Song, H. Shu, G. Zhao, X. Lv, W. Xie, *Spectrochim. Acta, Part A* **2006**, *65*, 333.
15 A. V. Londhe, B. Gupta, S. Kohli, P. Pardasani, R. T. Pardasani, *Z. Naturforsch., B: Chem. Sci.* **2006**, *61b*, 213.
16 R. T. Pardasani, P. Pardasani, S. K. Yadav, P. V. Bharatam, *J. Heterocycl. Chem.* **2003**, *40*, 557.
17 R. T. Pardasani, P. Pardasani, V. Chaturvedi, S. K. Yadav, A. Saxena, I. Sharma, *Heteroat. Chem.* **2003**, *14*, 36.
18 R. T. Pardasani, P. Pardasani, M. M. Agrawal, G. Mathur, *Indian J. Chem., Sect. B: Org. Chem. Incl. Med. Chem.* **2001**, *40B*, 518.
19 R. T. Pardasani, P. Pardasani, M. M. Agrawal, R. Ghosh, G. Mathur, S. K. Yadav, T. Mukherjee, *Heterocycl. Commun.* **2000**, *6*, 591.
20 M. J. Frisch, G. W. Trucks, H. B. Schlegel, G. E. Scuseria, M. A. Robb, J. R. Cheeseman, V. G. Zakrzewski, J. A. Montgomery, Jr., R. E. Stratmann, J. C. Burant, S. Dapprich, J. M. Millam, A. D. Daniels, K. N. Kudin, M. C. Strain, O. Farkas, J. Tomasi, V. Barone, M. Cossi, R. Cammi, B. Mennucci, C. Pomelli, C. Adamo, S. Clifford, J. Ochterski, G. A. Petersson, P. Y. Ayala, Q. Cui, K. Morokuma, D. K. Malick, A. D. Rabuck, K. Raghavachari, J. B. Foresman, J. Cioslowski, J. V. Ortiz, B. B. Stefanov, G. Liu, A. Liashenko, P. Piskorz, I. Komaromi, R. Gomperts, R. L. Martin, D. J. Fox, T. Keith, M. A. Al-Laham, C. Y. Peng, A. Nanayakkara, C. Gonzalez, M. Challacombe, P. M. W. Gill, B. Johnson, W. Chen, M. W. Wong, J. L. Andres, C. Gonjalez, M. Head-Gordon, E. S. Replogle, J. A. Pople, *Gaussian 98, Revision A. 6.*, Gaussian Inc., Pittsburgh, PA, **1998**. http://www.Gaussian.com.
21 M. J. S. Dewar, E. G. Zoebisch, E. F. Healy, J. J. P. Stewart, *J. Am. Chem. Soc.* **1985**, *107*, 3902.
22 A. Furusaki, T. Watanabe, *Chem. Pharm. Bull.* **1973**, *21*, 931, and references therein.
23 T. Lanz, A. Tropf, F.-J. Marner, J. Schroder, G. Schroder, *J. Biol. Chem.* **1991**, *266*, 9971.
24 K. J. Falci, R. W. Franck, G. P. Smitht, *J. Org. Chem.* **1977**, *42*, 3317.
25 β-Lactam antibiotics for clinical use. *Clinical Pharmacology Series*, ed. by S. F. Queener, J. A. Webber, S. W. Queener, Marcel Dekker, New York, **1986**, Vol. 4.